

# LABEL-FREE IDENTIFICATION OF MYOPATHOLOGICAL FEATURES WITH COHERENT ANTI-STOKES RAMAN SCATTERING

DANIEL NIEDIEKER, PhD,<sup>1</sup> FREDERIK GROSSERÜSCHKAMP, PhD,<sup>1</sup> ANJA SCHREINER,<sup>2</sup> KATALIN BARKOVITS, PhD,<sup>3</sup> CARSTEN KÖTTING, PhD,<sup>1</sup> KATRIN MARCUS, PhD,<sup>3</sup> KLAUS GERWERT, PhD,<sup>1</sup> and MATTHIAS VORGERD, MD<sup>2</sup>

<sup>1</sup> Department of Biophysics, Ruhr-University Bochum, Bochum, Germany

<sup>2</sup> Neurological Clinic Bergmannsheil, Ruhr-University Bochum, Bochum, Germany

<sup>3</sup> Medizinisches Proteom-Center, Ruhr-University Bochum, Bochum, Germany

Accepted 30 March 2018

**ABSTRACT:** *Introduction:* The aim of this study was the label-free identification of distinct myopathological features with coherent anti-Stokes Raman scattering (CARS) imaging, which leaves the sample intact for further analysis. *Methods:* The protein distribution was determined without labels by CARS at 2,930 cm<sup>-1</sup> and was compared with the results of standard histological staining. *Results:* CARS imaging allowed the visualization of glycogen accumulation in glycogen storage disease type 5 (McArdle disease) and of internal nuclei in centronuclear myopathy. CARS identified an inhomogeneous protein distribution within muscle fibers in sporadic inclusion body myositis that was not shown with standard staining. In Duchenne muscular dystrophy, evidence for a higher protein content at the border of hypercontracted fibers was detected. *Discussion:* CARS enables the label-free identification of distinct myopathological features, possibly paving the way for subsequent proteomic, metabolic, and genomic analyses.

*Muscle Nerve* 58:456–459, 2018

**D**iagnosis of myopathies is generally based on clinical, biochemical, magnetic resonance imaging, histological, and genetic studies. Muscle biopsy is often important in the evaluation of patients with a suspected myopathy. Histological and histochemical staining, immunohistochemistry, and Western blotting are essential for the conventional evaluation of patients with suspected muscle diseases. These techniques cause irreversible changes to the sample, eliminating the possibility of further investigations of the tested tissue section. Because the biochemical and morphological composition of adjacent slices

can vary significantly, the investigation of small morphological features such as protein aggregates or nuclei is complicated.

Some shortcomings of conventional staining can be overcome by label-free coherent anti-Stokes Raman scattering (CARS). As a variant of the Raman effect,<sup>1</sup> CARS permits the label-free determination of the biochemical composition of tissues and, thus, permits visualization of morphological structures while leaving the sample unchanged and available for further analysis.<sup>2</sup> CARS imaging can also be used in addition to standard histological staining to visualize protein or lipid components. Furthermore, by combination with other label-free techniques, pseudo-hematoxylin and eosin (H&E) staining can be generated.<sup>2</sup> CARS is a nonlinear technique in which 3 coherently aligned laser beams are used to create a blueshifted anti-Stokes signal. The signal is enhanced if the energy difference of the pump and Stokes lasers matches the energy difference of vibrational energy states.<sup>1</sup> Thus, the CARS signal is highly specific for single molecules (Supp. Info. Fig. 1). In this proof-of-principle study, we performed label-free CARS measurements on muscle biopsies from patients with different myopathies to investigate the feasibility and possible role of muscle CARS in muscle histopathology.

## MATERIALS AND METHODS

**Conventional Histology.** Approval for this study was granted by the institutional review board of the Ruhr-University, Bochum. We included patients from our neuromuscular center Ruhrgebiet, which is a reference center for neuromuscular diseases. The muscle biopsies were analyzed in the neuropathological laboratory of the Department for Neurology, University Hospital. Muscle tissue sections were obtained from patients with McArdle disease, sporadic inclusion body myositis (sIBM), centronuclear myopathy (CNM), and Duchenne muscular dystrophy (DMD). For conventional histochemical techniques, 10- $\mu$ m-thick cryostat sections were stained with H&E, modified trichrome Gomori, periodic acid-Schiff (PAS), and reduced nicotinamide adenine dinucleotide dehydrogenase-tetrazolium reductase and examined with a Nikon (Tokyo, Japan) Eclipse NI-SSR brightfield microscope. Immunohistochemical staining was performed according to standard procedures.

**Coherent Anti-Stokes Raman Scattering.** The measurements of the protein distribution were performed on dried, native samples by using a commercial setup (TCS SP5

Additional supporting information may be found in the online version of this article.

**Abbreviations:** CARS, coherent anti-Stokes Raman scattering; CNM, centronuclear myopathy; DMD, Duchenne muscle dystrophy; GSD, glycogen storage disease; H&E, hematoxylin and eosin; IBM, inclusion body myositis; PAS, periodic acid-Schiff; RV, rimmed vacuoles; sIBM, sporadic IBM

**Keywords:** CARS; histopathology; muscle myopathy; Raman imaging; skeletal muscle

**Funding:** This research was supported by the Protein Research Unit Ruhr within Europe, Ministry of Innovation, Science and Research of North-Rhine Westphalia, Germany (to K.G.) and the Heimer-Foundation, Bielefeld (to M.V.).

**Conflicts of Interest:** The authors have no conflicts of interest related to this report.

**Correspondence to:** M. Vorgerd, Neurologische Universitätsklinik und Poliklinik, Berufsgenossenschaftliches Universitätsklinikum Bergmannsheil, Bürkle-de-la-Camp-Platz 1, 44789 Bochum, Germany; e-mail: matthias.vorgerd@bergmannsheil.de or to K. Gerwert, Department of Biophysics, Ruhr-University Bochum, Bochum, Germany; e-mail: gerwert@bph.rub.de

© 2018 Wiley Periodicals, Inc.  
Published online 16 April 2018 in Wiley Online Library (wileyonlinelibrary.com). DOI 10.1002/mus.26140

II CARS; Leica, Heidelberg, Germany). An HCX IRAPO L25X/0.95 W (Leica) objective was used to focus the laser beam on the sample. Intensity images at  $2,930\text{ cm}^{-1}$  (pump wavelength 810 nm, Stokes wavelength 1,064 nm) were measured within 34 s (pixel dwell time 32  $\mu\text{s}$ ,  $1024 \times 1024$  pixels, resolution 300 nm) with a laser power at the sample of 28 mW (pump) and 21 mW (Stokes).<sup>3</sup> H&E staining was performed afterward on the same slides.

## RESULTS

The patient group consisted of a 60-year-old man with glycogen storage disease (GSD) type V (McArdle disease), a 1-month-old boy with a CNM, a 3-year-old boy with DMD, and a 58-year-old woman with sIBM. The protein distribution of the transverse tissue sections from these patients was detected by CARS at  $2,930\text{ cm}^{-1}$ . The CARS measurements and the gold standard, H&E staining, were performed on the same slide, whereas adjacent slices were used for the other histological stains. In McArdle disease (Fig. 1A), conventional staining showed intracellular glycogen storage and a lack of myophosphorylase activity. Glycogen accumulation caused lower intensities in the CARS image. In the patient with CNM (Fig. 1B), H&E staining showed chronic myopathy with central nuclei in many fibers. Immunostaining for emerin (green) and spectrin (red) and 4',6-diamidino-2 phenylindole counterstaining (blue) were performed on a tissue slice adjacent to that used for CARS and revealed an increased number of central nuclei. The internal nuclei showed lower intensities in the CARS image. In IBM (Fig. 1C), H&E and trichrome staining showed fiber variability, some central nuclei, necrotic and regenerating fibers, some rimmed vacuoles, and endomysial inflammatory infiltrates. Protein aggregation at the borders of the muscle fibers was observed in the CARS image but not with the conventional stains. In DMD (Fig. 1D), H&E and trichrome staining showed dystrophic features, including variation in fiber size, necrotic muscle fibers, endomysial fibrosis, and hypercontracted muscle fibers. In immunofluorescence studies, many fibers demonstrated a reduction of dystrophin, and there was a complete loss of dystrophin in Western blot analysis (not shown). A higher protein distribution was found at the borders of hypertrophic fibers. These features could be observed in other myopathological diseases (Supp. Info. Fig. 2).

## DISCUSSION

In this proof-of-principle approach, we chose different myopathies with distinct myopathological features to show the potential of CARS for label-free morphological pattern recognition. CARS microscopy allows the visualization of the molecular fingerprint and morphology of tissue sections.<sup>4</sup> As a nonlinear technique, CARS is used mostly to detect

the lipid and protein distribution in cells and tissue. Because of its high spatial resolution, CARS is able to separate cellular compartments in cells.<sup>3,5</sup> Furthermore, CARS can be used to separate healthy and diseased tissue in skin cancer,<sup>6</sup> colon cancer,<sup>2,7</sup> and brain cancer<sup>8</sup> and has been used to investigate smooth muscle in the colon<sup>9</sup> and in blood vessels.<sup>10</sup>

GSD type 5 (McArdle disease) shows increased intracellular glycogen due to an enzyme defect of myophosphorylase.<sup>11</sup> Glycogen, a polysaccharide, contains few  $\text{CH}_3$  bonds, whereas muscle fibers contain many  $\text{CH}_3$  bonds. The increased amount of cytosolic glycogen can be visualized as lower intensities in CARS and corresponds to the PAS-positive glycogen deposits seen in conventional histopathological staining. Additional analysis of some features of the metabolic and proteomic profiles of GSD may be facilitated by CARS and may provide more insights into metabolic adaptor processes that may be relevant to the treatment of patients with GSD.

CNM is a genetically heterogeneous congenital myopathy, and its key histopathological feature is the displacement of nuclei in muscle cells. These centrally placed nuclei suggest that the primary pathology is an arrest of muscle fiber maturation at the myotube stage. In a CARS image, muscle cell nuclei correspond to small areas with less CARS intensity, indicating lower protein content than that of the muscle fibers. Fluorescence staining of serial sections with emerin monoclonal antibodies shows a normal inner nuclear membrane signal. The integrity of the nuclear membrane cannot be determined by CARS, but nuclei can be identified in label-free CARS images. To further investigate the role of centrally located nuclei in CNM, CARS may be helpful to identify pathologically placed nuclei in label-free tissue sections and to select these with laser capture microscopy for further qRNA and proteomic analysis. This information may provide new hints for the diagnosis of the genetically different CNM forms and may identify marker profiles relevant to CNM pathophysiology.

In IBM, small groups of atrophic fibers, endomysial inflammation, and fibers with structural changes and rimmed vacuoles (RV) are seen in conventional staining. IBM pathogenesis includes inflammatory factors and impaired endolysosomal degeneration. Recently, we showed that RV in IBM are composed of a large number of proteins; a large subset of these proteins was associated with protein folding and autophagy.<sup>12</sup> FYCO1 is an autophagic adaptor protein and one of the proteins enriched in RV. FYCO1 genetic variants are overrepresented in patients with IBM, thus indicating a new IBM risk allele. In this study, CARS imaging showed an inhomogeneous protein distribution inside some muscle fibers that was not seen in standard staining. This finding may

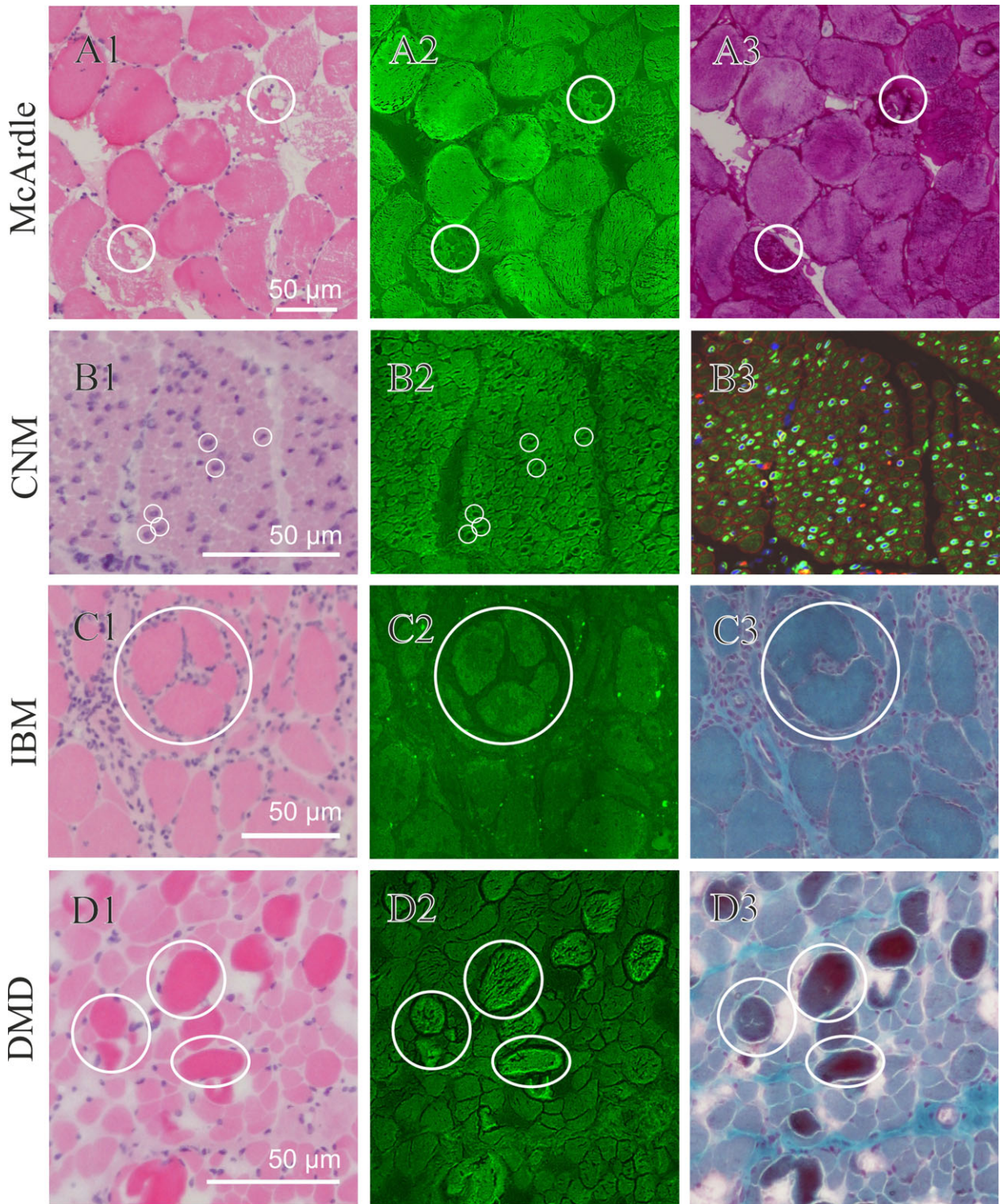


**FIGURE 1.** Comparison between CARS intensity images and images with different stains. Standard staining of glycogen storage disease type 5 (McArdle disease; **A**), centronuclear myopathy (**B**), inclusion body myositis (**C**), and DMD (**D**) were compared with label-free CARS intensity images (**middle column**). For standard staining, hematoxylin and eosin (**left column**), trichrome (**C3**), and periodic acid-Schiff (**A3**) were used. The intensity and localization of different specific proteins were investigated with immunostaining; the distribution of emerin (**B3**, green), dystrophin (**D3**, green), and spectrin (**B3**, red; **D3**, red) are depicted. 4',6-Diamidino-2 phenylindole counterstaining was used to mark nuclei (**B3**, blue). CARS, coherent anti-Stokes Raman scattering; CNM, centronuclear myopathy; DMD, Duchenne muscle dystrophy; IBM, inclusion body myositis.

indicate precursor protein aggregation, which is possibly relevant to the early pathogenesis of IBM. Additional studies of protein composition with CARS microscopy and mass spectrometry will permit analysis of the composition of these “early-onset” protein aggregates, which can then be compared with the known protein profiles of “downstream” aggregates in RV.<sup>13</sup> This approach is already established for infrared imaging.<sup>14</sup>

DMD is caused by mutations of the *dystrophin* gene, leading to dystrophic changes in muscle biopsies.<sup>15</sup> The dystrophin protein links the internal cytoskeleton to the extracellular membrane.<sup>16</sup> In label-free CARS imaging, we observed a higher protein content at the sarcolemma. This finding may reflect an upregulation of surrogate proteins in DMD. In addition, CARS showed some fibers with an increased signal corresponding to hypercontracted fibers in conventional staining. Ionized calcium overload as a causative factor in hypercontraction likely leads to an increased protein content in the affected fibers, which can be visualized by CARS.

In conclusion, this study shows the label-free recognition of myopathy features by using label-free CARS microscopy. This novel technology permits the label-free identification of distinct disease-specific features and allows subsequent next-generation sequencing, metabolomics, or proteomics in defined pathological areas of diseased skeletal muscle. This capability may be relevant not only to optimize the diagnostic workup but also to further improve techniques to study the molecular pathogenesis of acquired and hereditary myopathies.

The authors thank Lidia Janota for performing the histopathological staining.

Ethical Publication Statement: We confirm that we have read the Journal’s position on issues involved in ethical publication and affirm that this report is consistent with those guidelines.

## REFERENCES

1. Evans CL, Xie XS. Coherent anti-Stokes Raman scattering microscopy: chemical imaging for biology and medicine. *Annu Rev Anal Chem* 2008;1:883–909.
2. Bocklitz TW, Salah FS, Vogler N, Heuke S, Chernavskaja O, Schmidt C, *et al*. Pseudo-HE images derived from CARS/TPEF/SHG multimodal imaging in combination with Raman-spectroscopy as a pathological screening tool. *BMC Cancer* 2016;16:534.
3. El-Mashtoly SF, Niedieker D, Petersen D, Krauß SD, Freier E, Maghnoij A, *et al*. automated identification of subcellular organelles by coherent anti-Stokes Raman scattering. *Biophys J* 2014;106:1910–1920.
4. Krafft C, Schie IW, Meyer T, Schmitt M, Popp J. Developments in spontaneous and coherent Raman scattering microscopic imaging for biomedical applications. *Chem Soc Rev* 2016;45:1819–1849.
5. Klein K, Gigler AM, Aschenbrenner T, Monetti R, Bunk W, Jamitzky F, *et al*. Label-free live-cell imaging with confocal Raman microscopy. *Biophys J* 2012;102:360–368.
6. Breunig HG, Weinigel M, Bückle R, Kellner-Höfer M, Lademann J, Darvin ME, *et al*. Clinical coherent anti-Stokes Raman scattering and multiphoton tomography of human skin with a femtosecond laser and photonic crystal fiber. *Laser Phys Lett* 2013;10:25604.
7. Petersen D, Mavarani L, Niedieker D, Freier E, Tannapfel A, Kötting C, *et al*. Virtual staining of colon cancer tissue by label-free Raman micro-spectroscopy. *Analyst* 2017;142:1207–1215.
8. Galli R, Uckermann O, Temme A, Leipnitz E, Meinhardt M, Koch E, *et al*. Assessing the efficacy of coherent anti-stokes Raman scattering microscopy for the detection of infiltrating glioblastoma in fresh brain samples. *J Biophotonics* 2016;414:404–414.
9. Brackmann C, Esguerra M, Olausson D, Delbro D, Krettek A, Gatenholm P, *et al*. Coherent anti-Stokes Raman scattering microscopy of human smooth muscle cells in bioengineered tissue scaffolds. *J Biomed Optics* 2011;16(2):21115.
10. Wang HW, Le TT, Cheng JX. Label-free imaging of arterial cells and extracellular matrix using a multimodal CARS microscope. *Optics Commun* 2008;281:1813–1822.
11. Quinlivan R, Buckley J, James M, Twist A, Ball S, Duno M, *et al*. Mcardle disease: a clinical review. *J Neurol Neurosurg Psychiatry* 2010;81:1182–1188.
12. Guetsches AK, Brady S, Krause K, Maerkens A, Uszkoreit J, Eisenacher M, *et al*. Proteomics of rimmed vacuoles define new risk allele in inclusion body myositis. *Ann Neurol* 2017;81:227–239.
13. Kley RA, Maerkens A, Leber Y, Theis V, Schreiner A, Van der Ven PFM, *et al*. A combined laser microdissection and mass spectrometry approach reveals new disease relevant proteins accumulating in aggregates of filaminopathy patients. *Mol Cell Proteomics* 2013;12:215–227.
14. Großerueschkamp F, Bracht T, Diehl HC, Kuepper C, Ahrens M, Kal A, *et al*. Spatial and molecular resolution of diffuse malignant mesothelioma heterogeneity by integrating label-free FTIR imaging, laser capture microdissection and proteomics. *Sci Rep* 2017;7:1–12.
15. Deconinck N, Dan B. Pathophysiology of Duchenne muscular dystrophy: current hypotheses. *Pediatr Neurol* 2007;36:1–7.
16. Winder SJ. The membrane-cytoskeleton interface: the role of dystrophin and utrophin. *J Muscle Res Cell Motil* 1997;18:617–29.